

No growth stimulation of tropical trees by 150 years of CO₂ fertilization but water-use efficiency increased

Peter van der Sleen, Peter Groenendijk, Mart Vlam, Niels P.R. Anten, Arnoud Boom, Frans Bongers, Thijs L. Pons, Gideon Terburg and Pieter A. Zuidema

Content:

Supplementary Methods

Supplementary Tables 1 – 5

Supplementary Figures 1 – 6

Supplementary References

Supplementary Methods

Study areas

The study was carried out in undisturbed tropical forest areas on three continents (Fig. 1): Bolivia in South America, Thailand in Southeast Asia and Cameroon in Africa. In Bolivia, trees were collected in the logging concession 'La Chonta', around 300 km northeast of Santa Cruz de la Sierra (15.84 S, 62.85 W). The forest in La Chonta is a semi-deciduous moist forest and the transitional between Chiquitano dry forest and moist Amazonian forests¹. Annual precipitation in the region averages 1580 mm, with a 4 month dry season receiving <100 mm from May to September (Supplementary Fig. 6). In Thailand, trees were collected in the Huai Kha Khaeng Wildlife Sanctuary (HKK), Uthai Thani province, around 250 km northwest of Bangkok (15.60 N, 99.20 E). The vegetation in HKK is a semi-deciduous moist forest². Mean annual rainfall averages 1473 mm, with a 4-6 months dry season from November to April (Supplementary Fig. 6). In Cameroon, field work took place in Forest Management Unit 11.001 of Transformation REEF Cameroon (TRC). This area is adjacent to the northwest border of Korup National park, in South-western Cameroon (5.23 N, 9.10 E). The forest consists of a semi-deciduous lowland rainforest of the Guineo-Congolian type. Annual precipitation in the region averages around 4000mm, with a dry season from December to February (Supplementary Fig. 6). Long-term trends in precipitation and temperature have been studied in the countries where the study sites are located. In Bolivia, a detailed climatological study of meteorological data from local stations showed no clear long-term change of total annual precipitation (but possibly a drying trend since 1985) and an increase of annual average temperature of $\sim 0.1^{\circ}\text{C}$ per decade since 1960³. In Thailand, meteorological data from Nakhon Sawan, the closest station to the study site ($\sim 100\text{km}$ east of HKK), were analysed by Nock, et al. ⁴, who showed no trends in total annual precipitation from 1950-2010, but an increase of mean daily temperature of $\sim 0.2^{\circ}\text{C}$ per decade since 1950. In Cameroon, climate trends were studied based on local stations^{5,6} and gridded data⁷. These studies provide some evidence for a possible drying trend since 1970⁷ (but this is not generally supported by local station data⁵) and show only a slight increase of temperature of $\sim 0.02^{\circ}\text{C}$ per decade since 1960^{5,6}.

Study species and collection

At each site, we sampled trees of four species (Supplementary Table 1). Species were selected based on their abundance (we chose relatively common species) and the possession of clear annual growth rings. At each site, trees were collected in 145-300 ha of undisturbed forest, located in a larger area of undisturbed forest (Thailand) or a mixture of selectively logged and pristine forests (Cameroon and Bolivia). Thus, no strong edge effects of disturbances outside the study areas were expected. All trees larger than 5 cm diameter at breast height (dbh) were sampled in a 50 meter radius around a randomly assigned gps point. At each site, we used ~ 25 random points spread over the study area and collected around 100 trees per species (ranging in size from 5 to >100 cm dbh). This spatial sampling approach

ensured that samples from all species were obtained from the entire study area. If the target of 100 samples per species was not reached within the circular plots, we sampled in the entire study area or chose an adjacent area (for *Daniellia ogea* and *Terminalia ivorensis* in Cameroon). In Cameroon and Bolivia, a first round of selective logging took place in the study area at the time of sampling (no previous logging had taken place in any of the areas). At these sites, logging operations permitted the collection of stem discs for ~30% of the sampled trees. If no discs could be collected, 0.5-cm diameter cores were collected using an increment borer (Suunto, Finland and Haglöf, Sweden). Cores were taken in at least three different directions at breast height. After drying, the surface of discs and cores were either cut or polished depending on what gave the best visibility of ring boundaries.

Ring measurements, growth calculation and the quality of dating

Ring width was measured using a LINTAB 6 measuring table and TSAPWin software (Rinntech, Germany) or using high-resolution scans (1600 dpi) and WinDendro software (Regent Instruments, Canada). Ring widths were measured for each tree in at least three different directions following standard dendrochronological approaches⁸. Measured tree-ring widths were converted to growth in cross-sectional area of the tree (basal area increment, BAI), as this gives a good estimate of above-ground tree biomass growth⁹.

The annual nature of ring formation for the Bolivian species has been previously demonstrated by Lopez, et al.¹⁰. For the Thai species, this was done by Baker, et al.¹¹ and for our sampled trees by Vlam, et al.¹². For the species from Cameroon, Groenendijk, et al.¹³ evaluated annual ring formation of three of the study species using radio-carbon dating on samples included in this study. They found a high-quality dating for two of these species (*Brachystegia eurycoma* and *Daniellia ogea*), while the third (*Brachystegia cynometroides*) showed some discrepancy in dating, leading to an underestimation of tree ages by approximately 10%. Annual ring formation of the fourth Cameroonian study species (*Terminalia ivorensis*) was established by Detienne, et al.¹⁴ in Cameroon.

We checked the quality of the dating of tree rings in our sampled trees in two ways. (1) For each tree, we visually cross-dated (i.e. matched) the ring-width series across the three directions. Matching the ring-width series in different directions allows the detection of locally absent (missing) or false rings in many cases. This is standard practice in tree-ring research⁸ and was successfully done for all 1100 sampled trees. (2) For four of the 12 species, we constructed an overall (master) chronology for the study species and subsequently checked whether annual variation in ring-width of individual trees matched with the chronology. A tree-ring chronology describes the common annual variation in ring width of a group of trees and is usually applied to verify the dating of tree-ring series⁸. For tree species in (wet) tropical forests, it has proven difficult to establish (strong) chronologies, even when dating accuracy is high (e.g., Fichtler, et al.¹⁵). This is probably due to the lack of a dominant climatic effect on annual growth fluctuations in most trees. We stress that our study was not aimed at, nor designed to, establish (strong) chronologies: we included many small (juvenile) trees which often

poorly cross-date (but have nonetheless annual rings¹⁶), included a site with high precipitation and low seasonality (Cameroon) and did not select species based on their responsiveness to climate variation.

Nevertheless, master chronologies were successfully produced for the four Thai study species, and included close to 60% of the sampled trees¹². This result shows that at the Thai site annual climatic variation has a dominant effect in tree growth that is experienced by the majority of trees. At the Bolivian site, with similar annual rainfall and seasonality, it was not possible to establish high-quality chronologies that contained a substantial portion of the sampled individuals and exhibited high inter-series correlations. Finally, at the very wet site in Cameroon it proved difficult to construct chronologies for all study species¹³. We reiterate that lacking chronologies for most of our study species does not imply that the quality of ring dating in these species was low (c.f., Groenendijk, et al. ¹³; Fichtler, et al. ¹⁵). We also stress that for the purpose of our study – detecting trends in the intercellular CO₂ concentration in leaves (C_i), intrinsic water-use efficiency (iWUE) and basal area increment (BAI) over time – the accuracy of ring dating is of limited importance and that we used average values of five rings as input in our statistical analyses.

Possible dating errors in our tree-ring series may cause uncertainty in the ‘calendar year’ value that is used to evaluate trends in C_i , iWUE and BAI over time or may cause these ‘calendar year’ values to be shifted towards the recent or distant past if species predominantly present missing or false rings. Such uncertainty or shifts in ‘calendar year’ values may have changed the probability of finding trends in C_i , iWUE and BAI but unlikely changed the direction of such trends. To test the effect of dating errors, we reran all statistical analyses (mixed-effect models, see below under ‘Statistical analyses’) including a number of ‘likely’ and ‘extreme’ dating errors. We tested four dating error scenarios, in which the average dating error ranged from a 3% chance of misidentification per dated growth ring (i.e. leading, on average, to 3 wrongly identified growth rings per 100 years) to an extreme case of a 20% chance of misidentification per dated growth ring (i.e. leading, on average, to 20 wrongly identified growth rings per 100 years). To implement dating errors, we changed the ‘year’ value of each data point in our sample using one of four normal distributions of errors, with mean errors of 0.03, 0.05, 0.10 and 0.20, and standard deviation estimated based on radio carbon (¹⁴C) dating of Cameroonian study species (0.04 to 0.20)¹³. For each dating error scenario we repeated this procedure 100 times, each time rerunning the mixed effect models that were used to relate C_i , iWUE and BAI to ‘year’. For each of these analyses we thus obtained 100 p-values. We then checked the number of cases that these values shifted from being significant ($p < 0.05$) to non-significant or vice versa. A large proportion of such shifts would imply that the particular test is sensitive to dating errors. These bootstrap analyses showed that the results of our analyses are fully robust to dating errors, and even to extreme ones: in none of the cases the bootstrapped p-values shifted from < 0.05 to > 0.05 or vice versa (Supplementary Table 5). The positive errors tested simulate the inclusion of ‘false’ rings. We also tested negative errors (referring to ‘missing’ rings). This gave results in the

same ranges as given in Supplementary Table 5, i.e. no shifts of p-values in any case (data not shown).

For one of our Cameroonian study species (*B. cynometroides*), a radiocarbon study showed that tree age was underestimated by approximately 10%¹³. In order to assure that the relatively large dating errors in this species would not affect the overall results of our statistical analyses, we also performed the analyses without this species. Excluding *B. cynometroides* gave the same qualitatively results as those presented in Supplementary Table 2, i.e. a significant increase in C_i and iWUE over time and no significant change of tree growth over time. In short, it is highly unlikely that dating errors in our tree-ring data resulted in erroneous growth trends or prevented the detection of growth trends.

Correcting for ontogenetic changes in growth

Because diameter growth of trees changes with tree size (and age), it is important to separate ontogenetic growth changes from potential growth changes over time. We applied a modified version of the method proposed and implemented by Rozendaal, et al.¹⁷. That is, we compared growth rates in the years around two fixed diameters: understorey trees (8 cm dbh) and canopy trees (27 cm dbh). For canopy trees, we assessed changes in growth over time by selecting the ring formed when a tree reached the target size of 27 cm dbh. We did this for all trees that were sufficiently large (>27cm dbh). We measured this ‘central’ ring as well as the two rings formed before and after the central ring, and averaged the widths of these five rings. By using five rings, we obtained an estimate of tree growth that was only marginally affected by year-to-year variation in growth due to climatic fluctuations. As we collected trees ranging in size from 5 to >100 cm dbh, the rings formed around the 27 cm diameter differ in age and allow comparisons of growth rates over long time spans for trees of the same size (Fig. 3a). The same procedure was used for understorey trees, but then for a target dbh of 8 cm (Fig. 2a). A total of approximately 100,000 rings were measured to derive the age of the rings around the 8 and 27 cm diameter sections in the 1109 sampled trees. Around 9000 rings were used to calculate BAI of the two target sizes (8 and 27 cm dbh).

Stable carbon isotope analyses

The analysis of trends in the CO₂ concentration in the intercellular spaces (C_i) and intrinsic Water-Use Efficiency (iWUE) was done in a similar way as those for BAI, again using canopy and understorey trees. By using the same selected tree rings from which we obtained BAI values, we could directly compare physiological responses to elevated CO₂ levels with growth responses over the same period. We cut wood from the selected tree rings (around 8 and 27 cm dbh) and obtained 5-year bulk samples from which cellulose was extracted using a modification of the Jayme-Wise method¹⁸. Crude cellulose samples were subsequently homogenized in a demi-water solution by a mixer mill (Retsch MM301, Germany) and oven-dried at 60 °C. All cellulose samples were analysed in a continuous flow mode with an element analyser coupled to a mass spectrometer (Sercon Hydra 20-20) at Leicester

Environmental Stable Isotope Laboratory, University of Leicester, United Kingdom. The carbon isotope composition ($\delta^{13}\text{C}$, in ‰) was then calculated as:

$$\delta^{13}\text{C}_{\text{tree-ring}} = (R_{\text{sample}} / R_{\text{standard}} - 1) * 1000 \quad (1)$$

where R_{sample} is the $^{13}\text{C}/^{12}\text{C}$ ratio of a sample and R_{standard} the $^{13}\text{C}/^{12}\text{C}$ ratio of an internationally recognized standard material (V-PDB). Discrimination against the heavier ^{13}C ($\Delta^{13}\text{C}$) was calculated as:

$$\Delta^{13}\text{C} = (\delta^{13}\text{C}_a - \delta^{13}\text{C}_{\text{tree-ring}}) / (1 + \delta^{13}\text{C}_{\text{tree-ring}}) \quad (2)$$

where $\delta^{13}\text{C}_a$ is the $\delta^{13}\text{C}$ of atmospheric CO_2 (currently about -8.1‰). $\delta^{13}\text{C}_a$ decreased by 1.7‰ since the onset of the industrial revolution due to the burning of fossil fuels, which are depleted in ^{13}C . We used published data for $\delta^{13}\text{C}_a$ ^{19,20} to correct for this change. We then used Farquhar's model²¹ for the discrimination of ^{13}C in plants to estimate CO_2 concentration in the intercellular spaces of the leaves (C_i) from the discrimination values determined in equation 2:

$$\Delta^{13}\text{C} \approx a + (b - a) C_i / C_a \quad (3)$$

where a (4.4‰) refers to the slower diffusion of $^{13}\text{CO}_2$ compared to $^{12}\text{CO}_2$ through the stomata, and b (27‰) to the discrimination by the CO_2 fixing enzyme Rubisco. C_a is the CO_2 concentration of the atmosphere and was obtained from direct measurements of atmospheric CO_2 concentrations²². Intrinsic Water-Use Efficiency (iWUE), the rate of CO_2 assimilation (A) divided by the stomatal conductance for water vapour (g_s)²³, was estimated from C_i , as:

$$\text{iWUE} = A/g_s = (C_a - C_i)/1.6 \quad (4)$$

Note that $\delta^{13}\text{C}$ at the level of wood cellulose is not the same as at the level of primary assimilates because of downstream discrimination during transport and cellulose synthesis, which cause $\delta^{13}\text{C}$ values of cellulose in growth rings to be lower than the $\delta^{13}\text{C}$ of leaf sugars (about 1-2‰^{24,25}). $\Delta^{13}\text{C}$ does thus not represent real C_i and iWUE values, but can nonetheless be used to determine relative changes in C_i and hence iWUE.

Vapour Pressure Deficit

Trends in iWUE can represent trends in water-use efficiency (the ratio of assimilation to transpiration²³) if the vapour pressure (VP) difference between the air and inside the leaves remains constant. This VP difference can increase as a result of global warming and/or decreased precipitation

and lead to increased transpiration over time. To assess long-term changes of the VP difference between the air and inside the leaves, we checked if the vapour pressure deficit (VPD), the difference between actual VP and the saturated VP (VP_{sat}), has increased over the investigated period. We calculated VP_{sat} from maximum monthly air temperatures according to Allen, et al. ²⁶:

$$VP_{sat} = 0.6108 \text{ Exp } (17.27 T_{air}) / (T_{air} + 237.3) \quad (5)$$

Maximum monthly air temperature (T_{air}) over the period 1901 to 2009 for each study site were obtained from the CRUTS3.0 gridded dataset (University of East Anglia Climate Research Unit 2009). We used gridded data as long-term climate data are not available for two of our sites. To estimate VPD, we subtracted VP_{sat} from the actual VP over the period 1901-2009 for each study site (also from the gridded CRUTS3.0 dataset). We assumed that the VPD is representative for the VP difference between leaf and air, which is valid when the difference between air and leaf temperature does not change and the increase in temperature over the experimental period is small. However, this is not necessarily true if leaf cooling has changed as a result of decreasing transpiration with increasing CO_2 ²⁷. We calculated the average VPD during the growth season (October to May in Bolivia; March to December in Cameroon and May to December in Thailand) and used a regression analysis to detect changes in VPD over time (Supplementary Fig. 1).

Statistical analyses

We analysed long-term changes in intrinsic Water-Use Efficiency (iWUE) and Basal Area Increment (BAI) with a linear mixed-effect (LME) model and included ‘calendar year’ as a fixed factor and ‘tree species’ as a random factor in the analysis of trees per country and both ‘tree species’ and ‘country’ as random factors in the analysis of an overall pan-tropical trend (i.e. combining all trees measured). The natural logarithm was taken of C_i and iWUE to obtain linear relationships and for BAI to stabilize the variance. We tested two models: one with only random intercepts and one with both random intercepts and slopes. In all analyses, the model with both random intercepts and slopes was the most parsimonious, yielding the lowest Akaike’s Information Criteria (AIC). We performed the analyses for the 8 and 27 cm diameter trees separately.

We estimated the statistical power of the linear mixed-effect models to detect long-term changes in BAI. For each species a simulated dataset was created by randomly applying its de-trended variance in BAI to a certain positive slope (growth trend). Species were subsequently re-combined to generate a total dataset of 1109 virtual trees. We tested 20 growth trends ranging from an increase of 0.1 to 2% per decade from 1900-2010. For each trend, we generated 1000 datasets and for each of these datasets we tested if an LME model identical to the one used for the observed data detected a significant effect of ‘calendar year’. The number of case for which ‘calendar year’ was significant was divided by 1000

to obtain the estimated power of model and data to detect a given growth trend (Supplementary Fig. 3).

All analyses were performed in R, version 2.12.2, (R foundation for Statistical Computing, Vienna, Austria), using the package NLME.

The potential role of sampling biases

Studies of historical growth trends obtained from tree-ring measurements need to consider the potential influence of a number of sampling biases that can produce apparent but erroneous growth trends, or may mask actual growth trends induced by environmental changes^{17,28}. While there is still little evidence for the effects of sampling biases on growth trends derived from tree-ring studies²⁸, the potential effect of such biases clearly needs to be evaluated. Below, we discuss four sampling biases - three previously published^{28,29} and one additional bias ('juvenile selection effect') - and evaluate to what extent these may have led to erroneous growth trends or have erroneously masked growth trends. Supplementary Figure 2 illustrates these sampling biases.

Firstly, the 'big-tree selection bias' occurs when only the largest trees in a population are sampled, a common procedure in dendrochronological studies. As a result, slow-growing small trees are underrepresented in recent times as they did not reach the minimum sampling diameter²⁸. Such a sampling of trees could thus lead to an overestimation of tree growth in more recent decades, leading to an apparent long-term increase of tree growth over time (Supplementary Fig. 2b). As we included trees of all sizes in our sampling design, this bias could not have influenced our results.

A second hypothesized bias is the 'slow-grower survivorship' bias. If fast-growing individuals within a population live shorter, they are underrepresented in the ancient portion of the tree-ring dataset²⁸. Studies on temperate and tropical trees supports such a trade-off between growth rate and tree longevity^{30,31}. As a result of a shorter lifespan in fast-growing individuals, reconstructed growth rates in the distant past would be biased toward slower growth (i.e. large trees contain proportionally more slow growing individuals; Supplementary Fig. 2c), resulting in an apparent increasing growth trend. Our finding of no trends in tree growth over time in any of the sites is not consistent with the occurrence of this sampling bias, suggesting that 'slow-grower survivorship' effects are either very small or absent in our dataset.

A third bias is the 'pre-death slow growth bias' and is based on the slow growth that may occur in the years or decades preceding tree death²⁹. When growth rates are estimated from recently formed growth rings some slow-growing individuals may be actually in the 'process of dying'. For growth rates based on rings formed in a distant past (i.e. in extant large trees) this type of slow growth is absent because the trees used in the sample have all survived to the present day. As a consequence, this bias might lead to an apparent growth decrease over time²⁹ or it may mask a positive growth trend (Supplementary Fig. 2d). To prevent this bias from affecting our results, we re-ran all analyses excluding samples from the last 10 years, thus removing trees for which recent growth rates may

present pre-death slow growth. In that way, any potential pre-death slow growth is removed from the dataset. These analyses yielded the same results as obtained with the entire dataset: no significant trends in growth at any of the sites and for both understorey and canopy trees (Supplementary Table 3).

The fourth potential bias - the 'juvenile selection bias' - has not been described previously although the ecological phenomenon that fast-growing (very) small trees have a higher chance of reaching the canopy than slow growers was observed for temperate³² and tropical tree species¹⁷ ('juvenile selection effect'). Such differences in survival of small trees are likely caused by variation in light conditions and the resulting differences in growth rate and time required to pass the high-mortality sapling phase. The juvenile selection effect implies that large canopy trees of today were relatively fast growers as small trees (Supplementary Fig. 2e). In that case, growth of small trees realized in the distant past (i.e. in extant large trees) would, on average, be higher than that of small trees in the recent past (i.e. in extant small trees), because the slow growers in the distant past have been partially 'removed' from the population, while they are still present in the population of extant small trees. Therefore, the juvenile selection effect would result in an apparent trend of decreasing growth of small trees or may mask a positive growth trend induced by environmental changes. In our study, this bias may have influenced growth trends for small understorey trees (8 cm dbh). However, such a selection effect of fast growers is unlikely to occur in large canopy trees that have passed the high-mortality understorey phase, but there is a possibility that fast-growing canopy trees experience a lower mortality risk than slow growers. We therefore evaluated evidence for this bias in both the 8 and 27-cm dbh trees.

The premise is that the juvenile selection bias gradually 'removes' slow growers from the population. To test if a juvenile selection bias was present, we evaluated the trends in the growth rates of slow growers over time. The juvenile selection bias would result in a negative trend of the growth rate of slow growers over time. We applied a linear mixed-effect model on the slowest growing 25% of the sampled trees. For each species we first selected the slowest growing 25% of the individuals per decade. We then combined all species into one mixed-effect model (similar to all other analyses performed) to evaluate temporal trends in BAI of the 25% slowest growers, using 'calendar year' as a fixed factor and 'tree species' and 'country' as random factors. We performed this analysis for understorey and canopy trees separately. This approach is equivalent to a quantile regression for the 25th percentile, but has the advantage of including random effects. For both understorey and canopy trees, we found no significant trends in BAI of slow growers over time (Supplementary Table 4). These analyses therefore provide no evidence for an underrepresentation of slow-growing individuals in the distant past. Thus, it is unlikely that a juvenile selection bias has erroneously masked a positive growth trend in our tree-ring data.

Supplementary Table 1. | The tree species studied.

Country	Species	Family	Functional group ¹	Phenology ²	Ring boundary ³	Annual rings
Bolivia	<i>Ampelocera ruizii</i>	Ulmaceae	ST	Evergreen	Marginal parenchyma	10
	<i>Cariniana ianeirensis</i>	Lecythidaceae	PST	Deciduous	Compressed fibres	10
	<i>Hura crepitans</i>	Euphorbiaceae	PST	Deciduous	Compressed fibres	10
	<i>Sweetia fruticosa</i>	Fabaceae	LLP	Brevi-deciduous	Marginal parenchyma	33
	<i>Brachystegia cynometroides</i>	Fabaceae	PST	Brevi-deciduous	Marginal parenchyma	13*
Cameroon	<i>Brachystegia eurycoma</i>	Fabaceae	PST	Brevi-deciduous	Marginal parenchyma	13
	<i>Daniellia ogea</i>	Fabaceae	PST	Brevi-deciduous	Marginal parenchyma	13
	<i>Terminalia ivorensis</i>	Combretaceae	LLP	Deciduous	Variation in wood density	14
	<i>Afzelia xylocarpa</i>	Fabaceae	LLP	Deciduous	Marginal parenchyma	11,12
	<i>Chukrasia tabularis</i>	Meliaceae	PST	Evergreen/ Brevi-deciduous	Marginal parenchyma	11,12
Thailand	<i>Melia azedarach</i>	Meliaceae	LLP	Deciduous	Ring porous	11,12
	<i>Toona ciliata</i>	Meliaceae	LLP	Deciduous	Ring porous	11,12

¹ Functional groups are based on the definitions in Poorter, et al. ³⁴: ST=shade-tolerant, PST=partial shade-tolerant, LLP=long-lived pioneer.

² Data on leaf phenology are from Mostacedo, et al. ³⁵ for the Bolivian species; Williams, et al. ³⁶ for the Thai species; Lemmens, et al. ³⁷ and Poorter, et al. ³⁸ for the Cameroonian species.

³ Ring boundary categories after Worbes ³⁹, classification based on personal observations.

* Dating of this species proved difficult because of the high percentage of missing and false rings, leading to a 10% underestimation of tree age¹³. A mixed-effect model without *B. cynometroides* yielded qualitatively the same results as those presented in Supplementary Table 2, i.e. a significant increase in C_i and $iWUE$ over time and no significant change of tree growth over time.

Supplementary Table 2. | Linear mixed-effect model results for canopy trees (27cm dbh) and understorey trees (8 cm dbh) . We analysed long-term changes in the CO₂ concentration in the intercellular spaces of leaves (C_i), intrinsic water-use efficiency (iWUE) and basal area increment (BAI), using ‘calendar year’ as a fixed factor (A) or ‘atmospheric CO₂ concentration (C_a)’ as a fixed factor (B). In both analyses, ‘tree species’ was inserted as a random factor when trees per country were studied or ‘tree species’ and ‘country’ were random factors in the study of an overall pan-tropical trend (i.e. combining all trees measured). The natural logarithm was taken of C_i, iWUE and BAI to obtain linear relationships and to stabilize the variance. We tested two models: one with only random intercepts and one with both random intercepts and slopes. In all analyses, the model with random intercepts and slopes was the most parsimonious, yielding the lowest Akaike’s Information Criteria (AIC).

A

C _i		Canopy trees					Understorey trees				
		Estimate	SE	df	t-value	p-value	Estimate	SE	df	t-value	p-value
All sites	Intercept	0.1143	0.4595	798	0.2487	0.8037	0.9869	0.5491	979	1.7974	0.0726
	Year	0.0026	0.0002	798	11.2069	<0.0001	0.0022	0.0003	979	7.9783	<0.0001
Bolivia	Intercept	-0.8159	0.6180	183	-1.3201	0.1884	0.6486	0.3177	339	2.0414	0.0420
	Year	0.0031	0.0003	183	9.6182	<0.0001	0.0024	0.0002	339	16.1018	<0.0001
Cameroon	Intercept	0.6812	0.3570	357	1.9080	0.0572	2.0627	0.8759	359	2.3550	0.0191
	Year	0.0024	0.0002	357	13.6833	<0.0001	0.0017	0.0005	359	3.6664	0.0003
Thailand	Intercept	0.1103	0.5197	256	0.2122	0.8321	0.6306	0.6830	279	0.9233	0.3566
	Year	0.0026	0.0003	256	9.5831	<0.0001	0.0024	0.0003	279	6.9171	<0.0001
iWUE		Canopy trees					Understorey trees				
		Estimate	SE	df	t-value	p-value	Estimate	SE	df	t-value	p-value
All sites	Intercept	0.7206	0.6125	798	1.1766	0.2397	1.0792	0.6424	979	1.6800	0.0933
	Year	0.0019	0.0003	798	5.7371	<0.0001	0.0016	0.0003	979	4.9554	<0.0001
Bolivia	Intercept	0.6624	0.6060	183	1.0931	0.2758	-0.0103	1.0492	339	-0.0098	0.9922
	Year	0.0019	0.0003	183	6.1569	<0.0001	0.0021	0.0005	339	4.2875	<0.0001
Cameroon	Intercept	1.5335	0.4383	357	3.4986	0.0005	1.7932	0.9638	359	1.8605	0.0636
	Year	0.0014	0.0002	357	5.9745	<0.0001	0.0012	0.0005	359	2.3570	0.0190
Thailand	Intercept	-0.8987	0.7945	256	-1.1312	0.2590	1.0886	0.8200	279	1.3276	0.1854
	Year	0.0027	0.0004	256	7.0548	<0.0001	0.0016	0.0004	279	4.0234	0.0001
BAI		Canopy trees					Understorey trees				
		Estimate	SE	df	t-value	p-value	Estimate	SE	df	t-value	p-value
All sites	Intercept	5.7648	2.5289	798	2.2796	0.0229	3.7063	3.1653	979	1.1709	0.2419
	Year	-0.0012	0.0013	798	-0.9022	0.3672	-0.0009	0.0016	979	-0.5668	0.5710
Bolivia	Intercept	6.0552	2.5897	183	2.3382	0.0205	2.0601	1.9440	339	1.0597	0.2900
	Year	-0.0015	0.0013	183	-1.1209	0.2638	-0.0001	0.0010	339	-0.1468	0.8834
Cameroon	Intercept	5.0374	4.4369	357	1.1353	0.2570	2.1715	3.7071	359	0.5858	0.5584
	Year	-0.0008	0.0023	357	-0.3328	0.7395	-0.0002	0.0020	359	-0.0805	0.9359
Thailand	Intercept	5.6418	4.9566	256	1.1383	0.2561	10.0827	5.1494	279	1.9580	0.0512
	Year	-0.0010	0.0024	256	-0.4105	0.6818	-0.0040	0.0025	279	-1.6035	0.1100

B

C_i		Canopy trees					Understorey trees				
		Estimate	SE	df	t-value	p-value	Estimate	SE	df	t-value	p-value
All sites	<i>Intercept</i>	4.2032	0.0491	798	85.5921	<0.0001	4.2925	0.0565	979	75.9289	<0.0001
	<i>Ca</i>	0.0033	0.0002	798	17.5814	<0.0001	0.0033	0.0002	979	21.5994	<0.0001
Bolivia	<i>Intercept</i>	4.1870	0.0844	183	49.5827	<0.0001	4.3636	0.1195	339	36.5241	<0.0001
	<i>Ca</i>	0.0034	0.0002	183	15.4746	<0.0001	0.0032	0.0002	339	13.5229	<0.0001
Cameroon	<i>Intercept</i>	4.1467	0.0361	357	114.7548	<0.0001	4.3510	0.1577	359	27.5849	<0.0001
	<i>Ca</i>	0.0036	0.0001	357	29.2188	<0.0001	0.0032	0.0006	359	5.4747	<0.0001
Thailand	<i>Intercept</i>	4.2966	0.0661	256	64.9787	<0.0001	4.2456	0.0915	279	46.3752	<0.0001
	<i>Ca</i>	0.0029	0.0002	256	18.6027	<0.0001	0.0034	0.0002	279	14.2275	<0.0001
iWUE		Canopy trees					Understorey trees				
		Estimate	SE	df	t-value	p-value	Estimate	SE	df	t-value	p-value
All sites	<i>Intercept</i>	3.6210	0.0719	798	50.368	<0.0001	3.4256	0.1238	979	27.667	<0.0001
	<i>Ca</i>	0.0023	0.0003	798	7.6472	<0.0001	0.0023	0.0004	979	6.6039	<0.0001
Bolivia	<i>Intercept</i>	3.7035	0.1318	183	28.107	<0.0001	3.2987	0.2374	339	13.893	<0.0001
	<i>Ca</i>	0.0019	0.0004	183	4.3797	<0.0001	0.0025	0.0005	339	5.2344	<0.0001
Cameroon	<i>Intercept</i>	3.6813	0.0647	357	56.936	<0.0001	3.3100	0.3554	359	9.3416	<0.0001
	<i>Ca</i>	0.0019	0.0002	357	8.6644	<0.0001	0.0026	0.0012	359	2.1102	0.0355
Thailand	<i>Intercept</i>	3.4731	0.1015	256	34.229	<0.0001	3.5006	0.1312	279	26.689	<0.0001
	<i>Ca</i>	0.0029	0.0003	256	10.641	<0.0001	0.0023	0.0003	279	6.7243	<0.0001
BAI		Canopy trees					Understorey trees				
		Estimate	SE	df	t-value	p-value	Estimate	SE	df	t-value	p-value
All sites	<i>Intercept</i>	3.8792	0.5288	798	7.3363	<0.0001	2.3882	0.7963	979	2.9991	0.0028
	<i>Ca</i>	-0.0012	0.0016	798	-0.7507	0.4531	-0.0013	0.0021	979	-0.6178	0.5368
Bolivia	<i>Intercept</i>	3.7593	1.1113	183	3.3827	0.0009	1.3204	1.0549	339	1.2516	0.2116
	<i>Ca</i>	-0.0016	0.0035	183	-0.4662	0.6416	0.0012	0.0029	339	0.4263	0.6701
Cameroon	<i>Intercept</i>	3.3398	0.8435	357	3.9564	0.0001	2.0514	1.0466	359	1.9599	0.0508
	<i>Ca</i>	0.0005	0.0030	357	0.1645	0.8694	-0.0006	0.0037	359	-0.1683	0.8664
Thailand	<i>Intercept</i>	4.1651	0.9804	256	4.2485	<0.0001	3.9019	1.0055	279	3.8806	0.0001
	<i>Ca</i>	-0.0014	0.0024	256	-0.6174	0.5375	-0.0049	0.0021	279	-2.3135	0.0214

Supplementary Table 3. | Accounting for the pre-death slow growth bias. The ‘pre-death slow growth bias’ may affect the detection of growth trends when recent growth rates are influenced by slow growth that could occur in the years or decades preceding tree death. Estimates of recent growth (of extant small trees) may then be biased towards lower values compared to those of extant large trees (see grey area in Supplementary Fig. 2d). To account for this bias, we excluded samples from the last 10 years (2010-2000) from the data set. The resulting mixed-effect model analyses yielded the same results as were obtained with the entire data set (Supplementary Table 2): no significant trends in basal area increment at any of the sites and for both understorey and canopy trees.

		Canopy trees					Understorey trees				
		Estimate	SE	df	t-value	p-value	Estimate	SE	df	t-value	p-value
All sites	<i>Intercept</i>	4.0944	2.4128	661	1.6969	0.0902	3.3780	2.1838	919	1.5469	0.1222
	<i>Year</i>	-0.0003	0.0012	661	-0.2534	0.8000	-0.0007	0.0011	919	-0.6544	0.5130
Bolivia	<i>Intercept</i>	0.4614	3.0502	111	0.1513	0.8800	2.9778	2.0877	279	1.4263	0.1549
	<i>Year</i>	0.0014	0.0016	111	0.9083	0.3657	-0.0006	0.0011	279	-0.5656	0.5721
Cameroon	<i>Intercept</i>	6.1204	4.8611	339	1.2591	0.2089	1.7283	3.2717	367	0.5282	0.5977
	<i>Year</i>	-0.0013	0.0026	339	-0.5230	0.6013	0.0001	0.0018	367	0.0409	0.9674
Thailand	<i>Intercept</i>	4.6891	5.0906	209	0.9211	0.3580	8.9511	6.0553	271	1.4782	0.1405
	<i>Year</i>	-0.0005	0.0025	209	-0.1990	0.8424	-0.0034	0.0029	271	-1.1501	0.2511

Supplementary Table 4. | Testing for evidence of a juvenile selection bias. We tested if slow-growing juvenile trees are gradually lost from the population (see grey area in Supplementary Fig. 2e), the ‘the juvenile selection bias’. This bias could have masked a CO₂-induced positive growth trend over time. To this end, we used a linear mixed-effect model on the slowest growing 25% of the sampled trees over time and performed this analysis for both canopy and understorey trees. We found no significant effect of calendar year in any of the analyses, i.e. slow-growing individuals are not underrepresented in the distant past. Thus, it is unlikely that juvenile selection biases have erroneously masked a positive growth trend in our dataset.

		Canopy trees					Understorey trees				
		Estimate	SE	df	t-value	p-value	Estimate	SE	df	t-value	p-value
All sites	<i>Intercept</i>	7.524	3.335	198	2.256	0.025	5.794	2.800	246	2.069	0.040
	<i>Year</i>	-0.002	0.002	198	-1.383	0.168	-0.002	0.001	246	-1.551	0.122
Bolivia	<i>Intercept</i>	6.321	6.193	46	1.021	0.313	7.620	4.611	86	1.653	0.102
	<i>Year</i>	-0.002	0.003	46	-0.580	0.565	-0.003	0.002	86	-1.371	0.174
Cameroon	<i>Intercept</i>	7.387	5.107	88	1.446	0.152	2.995	5.683	91	0.527	0.600
	<i>Year</i>	-0.002	0.003	88	-0.852	0.397	-0.001	0.003	91	-0.298	0.767
Thailand	<i>Intercept</i>	14.240	12.715	62	1.120	0.267	9.243	5.085	67	1.818	0.074
	<i>Year</i>	-0.006	0.006	62	-0.878	0.384	-0.004	0.002	67	-1.584	0.118

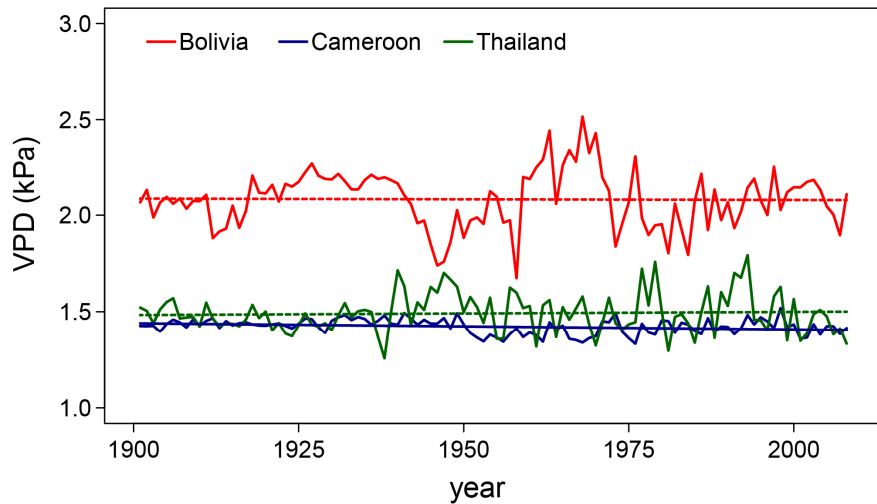
Supplementary Table 5. | Results of a bootstrapping analysis to assess the effect of dating errors. We tested the effect of dating errors by re-running all statistical analyses 100 times for each of four dating error scenarios, with increasing mean and standard deviation of dating errors. These errors were randomly assigned to each data point following a normal distribution with a mean value ranging from 0.03 to 0.20, and a standard deviation ranging from 0.04 to 0.2 (see ‘Ring measurements, growth calculation and the quality of dating’). A mean dating error of 0.03 (or 3%) implies that, on average, 3 out of 100 growth rings were wrongly identified. The positive errors tested, simulate the inclusion of ‘false’ rings. We also tested negative errors (referring to ‘missing’ rings). This gave results in the same ranges as for positive errors, i.e. no shifts in p-values from <0.05 to >0.05 or vice versa in any of the cases (data not shown).

A. understorey trees

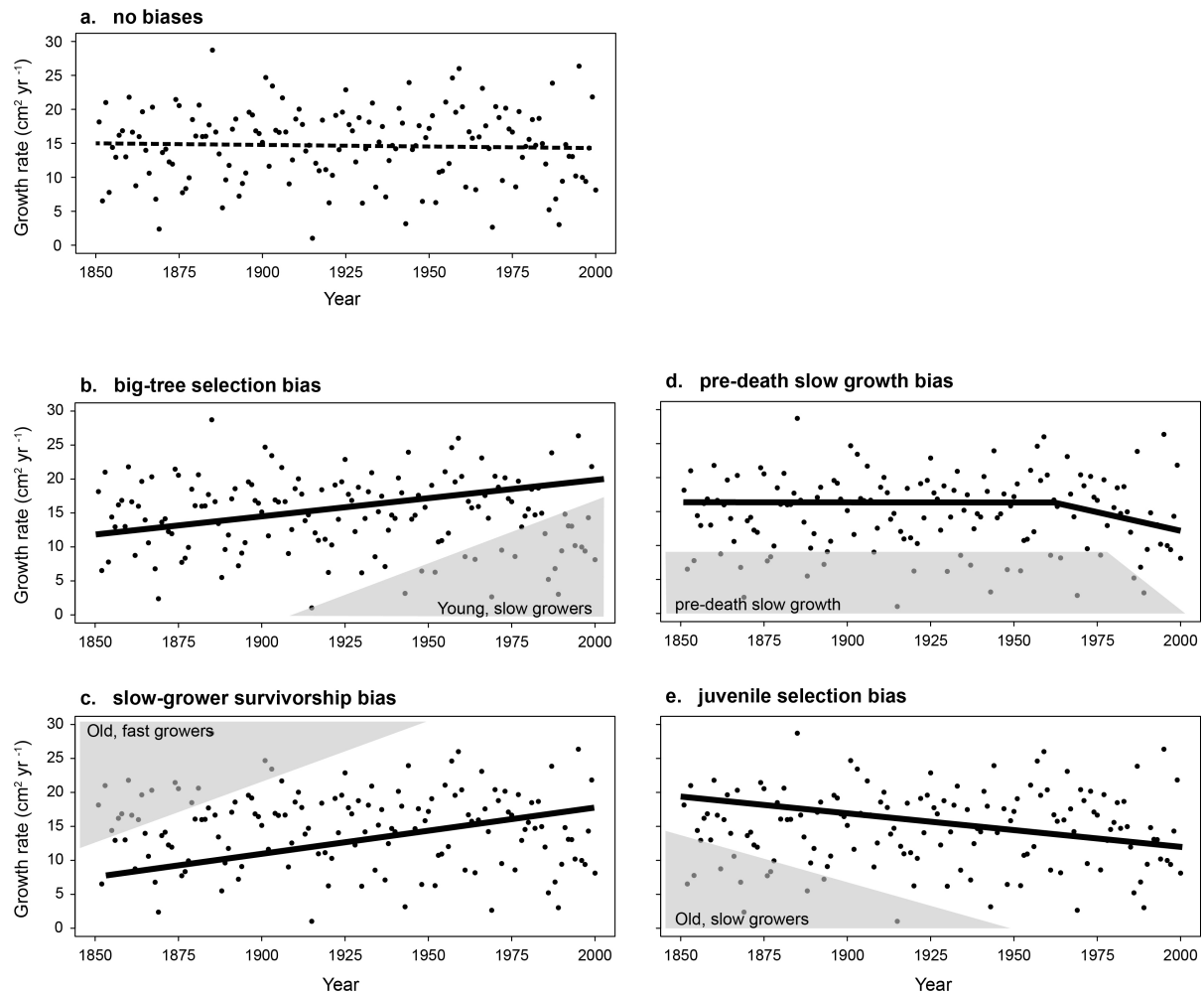
Added dating error	Average p-value (range)		
	BAI	C_i	iWUE
mean=0/stdev=0	0.571	<0.0001	<0.0001
mean=0.03/stdev=0.04	0.573 (0.521-0.628)	<0.0001 (<0.0001-<0.0001)	<0.0001 (<0.0001-<0.0001)
mean=0.05/stdev=0.05	0.574 (0.495-0.658)	<0.0001 (<0.0001-<0.0001)	<0.0001 (<0.0001-<0.0001)
mean=0.10/stdev=0.10	0.562 (0.409-0.769)	<0.0001 (<0.0001-<0.0001)	<0.0001 (<0.0001-0.0001)
mean=0.20/stdev=0.20	0.511 (0.386-0.672)	<0.0001 (<0.0001-<0.0001)	0.0017 (0.0013-0.0021)

B. canopy trees

Added dating error	Average p-value (range)		
	BAI	C_i	iWUE
mean=0/stdev=0	0.367	<0.0001	<0.0001
mean=0.03/stdev=0.04	0.368 (0.334-0.423)	<0.0001 (<0.0001-<0.0001)	<0.0001 (<0.0001-<0.0001)
mean=0.05/stdev=0.05	0.371 (0.311-0.415)	<0.0001 (<0.0001-<0.0001)	<0.0001 (<0.0001-<0.0001)
mean=0.10/stdev=0.10	0.382 (0.280-0.500)	<0.0001 (<0.0001-<0.0001)	<0.0001 (<0.0001-<0.0001)
mean=0.20/stdev=0.20	0.400 (0.215-0.654)	<0.0001 (<0.0001-<0.0001)	<0.0001 (<0.0001-0.0001)

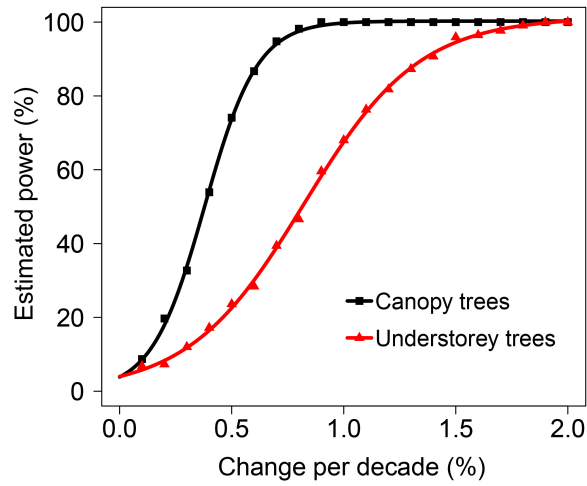


Supplementary Fig. 1. | Vapour pressure deficit (VPD) did not increase from 1901 to 2009 at the studied sites. Temporal trends in VPD were examined with a regression analyses. No trend in VPD was found in Bolivia and Thailand (dashed lines: $p < 0.05$), but a significant negative trend was found in Cameroon ($t = -2.769$, $p = 0.007$; solid line). We assumed that the VPD is representative for the VP difference between leaf and air, which is valid when the difference between air and leaf temperature does not change and the increase in temperature over the experimental period is small. These results indicate that the observed positive trends in *i*WUE (Figs. 2-3) represent positive trends in actual WUE, or underestimate such a trend for the Cameroon site.

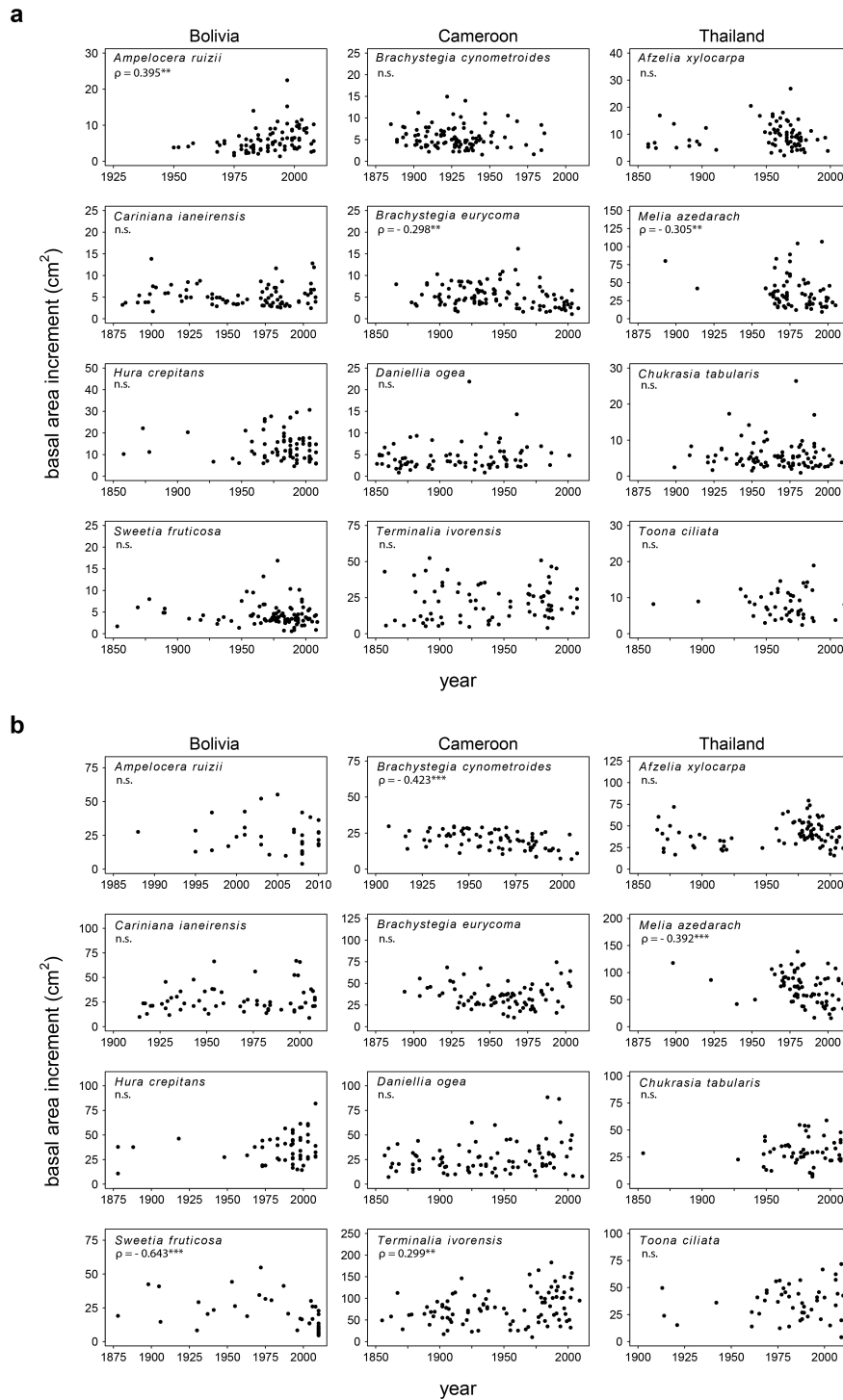


Supplementary Fig. 2. | Potential sampling biases in tree-ring research. Four sampling biases may create apparent (but erroneous) historical growth trends in tree-ring data or may mask actual growth trends induced by environmental changes. Data shown are randomly generated but comparable to growth data obtained in tree-ring studies such as ours. Growth rates are for trees of a particular size, e.g. the 8-cm and 27-cm diameter that we employed in this study (Fig. 2 and 3). **(a)** Historical tree growth rates from tree-ring data without sampling biases, showing no temporal trend in growth because growth values were generated for the same mean value over time. **(b)** The ‘big-tree selection bias’ occurs if only large trees are sampled. In that case ‘young, slow growing’ trees are likely underrepresented (grey area) because they did not reach the minimum sampling diameter. Recent growth rates will be overestimated, leading to a long-term growth increase (bold line). **(c)** The ‘slow-grower survivorship bias’ occurs if fast-growing trees live shorter than slow growers. Then, growth rates in the distant past will be biased towards slow growth, again leading to an apparent growth increase. **(d)** The ‘pre-death slow growth bias’ is based on the slow growth that may occur in the years or decades prior to the death of a tree. This type of growth could be included in the estimate of recent growth (based on recently formed growth rings) and thus bias it towards a lower value compared to growth rates based on rings formed in the distant past (in extant large trees). **(e)** The ‘juvenile selection bias’ can be considered as the reverse of the ‘slow-grower survivorship bias’ and could be relevant when the growth of juvenile trees is analysed over time. This bias is based on the possibility that fast-growing small trees have a higher chance of reaching the size at which

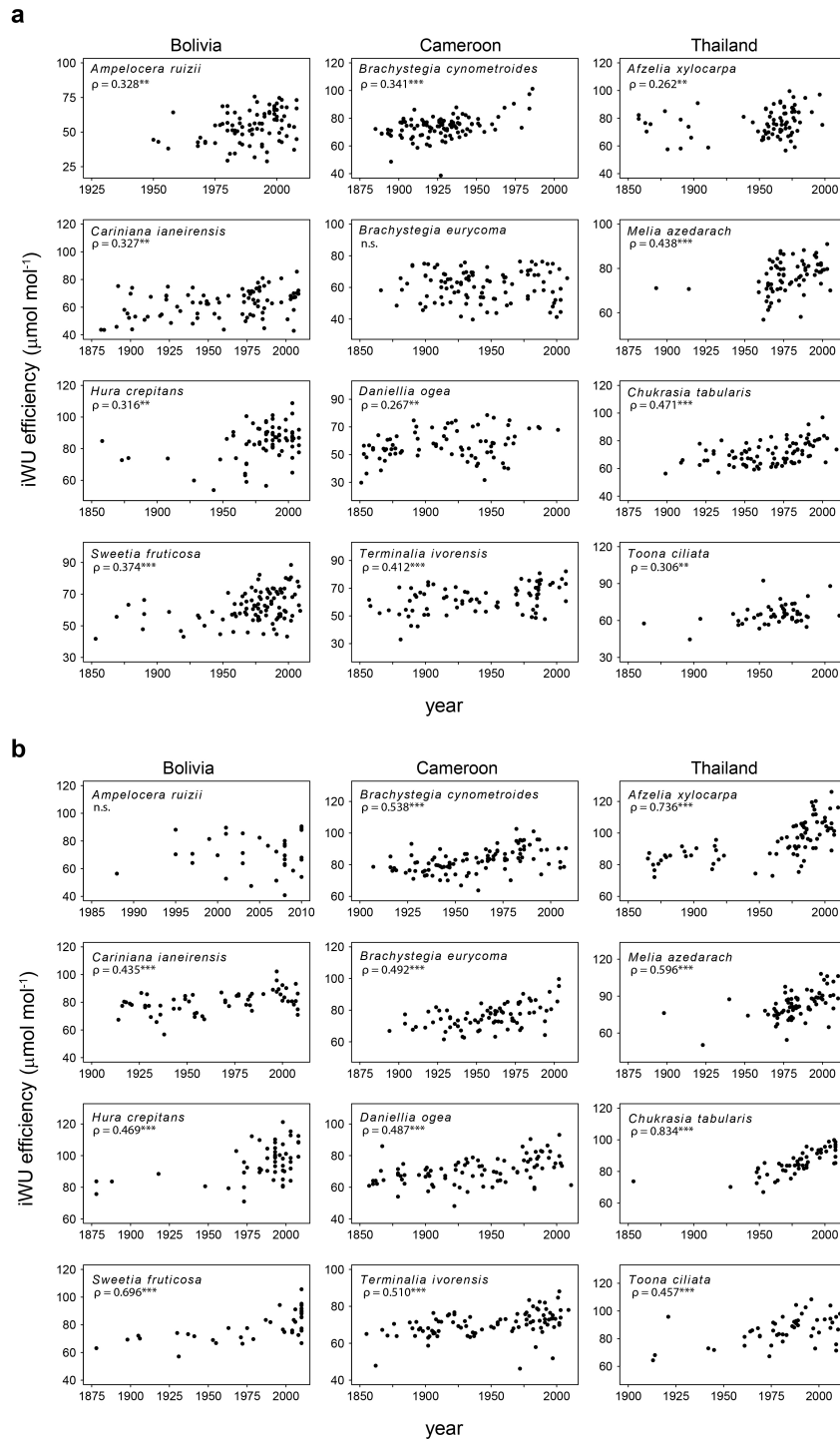
trees were sampled compared to slow growers¹⁷. If this is the case, there would be few slow-growing old trees and the growth of small trees realized in the distant past would be biased towards faster growth, leading to an apparent negative trend. Figure based on illustration in Brienen, et al.²⁸ and names of sampling biases follow those in that publication and in Bowman, et al.²⁹.



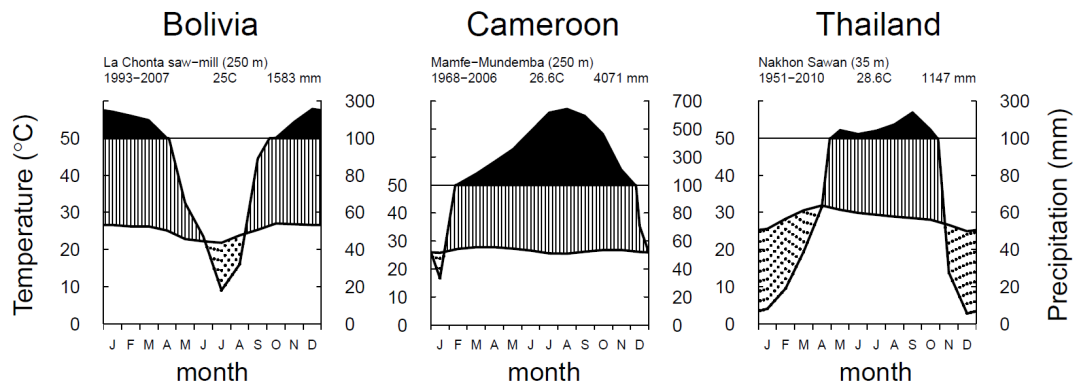
Supplementary Fig. 3. | The statistical power of the linear mixed-effect model to detect long-term changes in Basal Area Increment (BAI) when all study species are combined. We performed a power test to evaluate the probability of the mixed-effect model to detect varying growth trends (0.1 to 2% per decade from 1900 to 2010). We used simulated datasets based on the actual sample size and same variance structure as our observed data (see Supplementary Methods).



Supplementary Fig. 4. | Basal area increment over time per species. The shown basal area increment is the average annual increment over a 5-year period, i.e. based on 5 growth rings. Growth rates are compared over time for understorey trees (**a**) and canopy trees (**b**). Each point represents an individual tree (see methodology in Figs. 2a & 3a). Because the data are often skewed (with more samples in the recent past compared to the distant past), we used a non-parametric correlation (Spearman's rank correlation). Correlation coefficients (ρ) are given under the species name. Asterisks show to the level of significance (* $p < 0.05$, ** $p < 0.01$, *** $p < 0.001$). In only two cases a significant increase in tree growth was found (in 8 cm diameter *Ampelocera ruizii* and 27 cm *Brachystegia cynometroides*).



Supplementary Fig. 5. | Intrinsic water-use efficiency over time per species. The shown intrinsic water-use efficiency (iWUE) is the average over a 5-year period. iWUE is compared over time for understorey trees (a) and canopy trees (b). Each point represents an individual tree (see methodology in Figs. 2a & 3a). We used a non-parametric correlation (Spearman's rank correlation) to assess trends over time for each species. Correlation coefficients (ρ) are given under the species name. Asterisks show to the level of significance (* $p < 0.05$, ** $p < 0.01$, *** $p < 0.001$). For the CO_2 concentration in the intercellular spaces in leaves (C_i ; data shown in Figs. 2 and 3), a significant increase was found in both understorey and canopy trees for each species ($p < 0.0001$ in all cases).



Supplementary Fig. 6. | Climate diagrams for the study sites. For Bolivia, precipitation data are from the La Chonta saw-mill, located 30 km north of the study site. Temperature data are from Ascención de Guarayos (1987-2006), 60 km west of the study site. In Cameroon, monthly precipitation and temperature of two nearby stations were averaged: Mamfé Airport weather station (40 km north of study site) and Bulu meteorological station (40 km south of the study site). In Thailand precipitation and temperature data are for Nakhon Sawan, the closest station, 100 km east of the study site. The total annual precipitation at the Thai study site (HKK) is however higher than in Nakhon Sawan (around 1500 mm) and temperature lower ($23.5\text{ }^{\circ}\text{C}$)², but no long-term climate data are available for HKK. Dotted area indicates the dry season (precipitation <100 mm/month), black area the rainy season (<100 mm/month).

References

- 1 Peña-Claros, M. *et al.* Beyond reduced-impact logging: Silvicultural treatments to increase growth rates of tropical trees. *Forest Ecology and Management* **256**, 1458-1467 (2008).
- 2 Bunyavejchewin, S., LaFrankie, J. V., Baker, P. J., Davies, S. J. & Ashton, P. S. *CTFS Data Book Series. Forest trees of Huai Kha Khaeng Wildlife Sanctuary, Thailand.* (National Parks, Wildlife and Plant Conservation Department, 2009).
- 3 Seiler, C., Hutjes, R. W. A. & Kabat, P. Climate variability and trends in Bolivia. *Journal of Applied Meteorology and Climatology* **52**, 130-146 (2013).
- 4 Nock, C. A. *et al.* Long-term increases in intrinsic water-use efficiency do not lead to increased stem growth in a tropical monsoon forest in western Thailand. *Global Change Biology* **17**, 1049-1063 (2011).
- 5 Molua, E. L. Climate trends in Cameroon: implications for agricultural management. *Climate Research* **30**, 255-262 (2006).
- 6 Malhi, Y. & Wright, J. Spatial patterns and recent trends in the climate of tropical rainforest regions. *Philosophical Transactions of the Royal Society B: Biological Sciences* **359**, 311-329 (2004).
- 7 Asefi-Najafabady, S. & Saatchi, S. Response of African humid tropical forests to recent rainfall anomalies. *Philosophical Transactions of the Royal Society B: Biological Sciences* **368**, 20120306 (2013).
- 8 Stokes, M. A. & Smiley, T. L. *An introduction to tree-ring dating.* (University of Arizona Press, 1996).
- 9 Baker, T. R. *et al.* Increasing biomass in Amazonian forest plots. *Philosophical Transactions of the Royal Society B: Biological Sciences* **359**, 353-365 (2004).
- 10 Lopez, L., Villalba, R. & Peña-Claros, M. Determining the annual periodicity of growth rings in seven tree species of a tropical moist forest in Santa Cruz, Bolivia. *Forest Systems* **21**, 508-514 (2012).
- 11 Baker, P. J., Bunyavejchewin, S., Oliver, C. D. & Ashton, P. S. Disturbance history and historical stand dynamics of a seasonal tropical forest in western Thailand. *Ecological Monographs* **75**, 317-343 (2005).
- 12 Vlam, M., Baker, P. J., Bunyavejchewin, S. & Zuidema, P. A. Temperature and rainfall strongly drive temporal growth variation in Asian tropical forest trees. *Oecologia* **174**, 1449-1461 (2014).
- 13 Groenendijk, P., Sass-Klaassen, U., Bongers, F. & Zuidema, P. A. Potential of tree-ring analysis in a wet tropical forest: a case study on 22 commercial tree species in Central Africa. *Forest Ecology and Management* **323**, 65-78 (2014).

- 14 Detienne, P., Oyono, F., Durrieu de Madron, L., Demarques, B. & Nasi, R. Série FORAFRI. Document 15. L'analyse de cernes: applications aux études de croissance de quelques essences en peuplements naturels de forêt dense africaine. (CIRAD-Forêt, Montpellier, France, 1998).
- 15 Fichtler, E., Clark, D. A. & Worbes, M. Age and long-term growth of trees in an old-growth tropical rain forest, based on analyses of tree rings and ^{14}C . *Biotropica* **35**, 306-317 (2003).
- 16 Soliz-Gamboa, C. C., Sandbrink, A. & Zuidema, P. A. Diameter growth of juvenile trees after gap formation in a Bolivian rainforest: responses are strongly species-specific and size-dependent. *Biotropica* **44**, 312-320 (2012).
- 17 Rozendaal, D. M. A., Brienens, R. J. W., Soliz-Gamboa, C. C. & Zuidema, P. A. Tropical tree rings reveal preferential survival of fast-growing juveniles and increased juvenile growth rates over time. *New Phytologist* **185**, 759-769 (2010).
- 18 Wieloch, T., Helle, G., Heinrich, I., Voigt, M. & Schyma, P. A novel device for the batch wise isolation of α -cellulose from small-amount wholewood samples. *Dendrochronologia* **29**, 115-117 (2011).
- 19 Keeling, R. F., Piper, S. C., Bollenbacher, A. F. & Walker, S. J. Monthly atmospheric $^{13}\text{C}/^{12}\text{C}$ isotopic ratios for 11 SIO stations. In Trends: A Compendium of Data on Global Change. *Carbon Dioxide Information Analysis Center, Oak Ridge National Laboratory, U.S. Department of Energy, Oak Ridge, Tenn., U.S.A.* (2010).
- 20 McCarroll, D. & Loader, N. J. Stable isotopes in tree rings. *Quaternary Science Reviews* **23**, 771-801 (2004).
- 21 Farquhar, G. D., O'Leary, M. H. & Berry, J. A. On the relationship between carbon isotope discrimination and intercellular carbon dioxide concentration in leaves. *Australian Journal of Plant Physiology* **9**, 121-137 (1982).
- 22 Dlugokencky, E. & Tans, P. NOAA/ESRL (www.esrl.noaa.gov/gmd/ccgg/trends/) (2013).
- 23 Ehleringer, J., Hall, A. & Farquhar, G. *Stable isotopes and plant carbon-water relations*. (Academic Press, 1993).
- 24 Gleixner, G., Danier, H. J., Werner, R. A. & Schmidt, H. L. Correlations between the ^{13}C content of primary and secondary plant products in different cell compartments and that in decomposing basidiomycetes. *Plant Physiology* **102**, 1287-1290 (1993).
- 25 Badeck, F. W., Tcherkez, G., Nogués, S., Piel, C. & Ghashghaie, J. Post-photosynthetic fractionation of stable carbon isotopes between plant organs - A widespread phenomenon. *Rapid Communications in Mass Spectrometry* **19**, 1381-1391 (2005).
- 26 Allen, R. G., Pereira, L. S., Raes, D. & Smith, M. Crop Evapotranspiration: Guidelines for Computing Crop Water Requirements. (FAO Irrigation and drainage paper 56 Rome, Italy, 1998).

- 27 Cernusak, L. A. *et al.* Tropical forest responses to increasing atmospheric CO₂: current knowledge and opportunities for future research. *Functional Plant Biology* **40**, 531-551 (2013).
- 28 Brienen, R. J. W., Gloor, E. & Zuidema, P. A. Detecting evidence for CO₂ fertilization from tree ring studies: The potential role of sampling biases. *Global Biogeochemical Cycles* **26**, GB1025 (2012).
- 29 Bowman, D. M. J. S., Brienen, R. J. W., Gloor, E., Phillips, O. L. & Prior, L. D. Detecting trends in tree growth: Not so simple. *Trends in Plant Science* **18**, 11-17 (2013).
- 30 Bigler, C. & Veblen, T. T. Increased early growth rates decrease longevities of conifers in subalpine forests. *Oikos* **118**, 1130-1138 (2009).
- 31 Schöngart, J., Piedade, M. T. F., Wittmann, F., Junk, W. J. & Worbes, M. Wood growth patterns of *Macaranga acaciifolium* (Benth.) Benth. (Fabaceae) in Amazonian black-water and white-water floodplain forests. *Oecologia* **145**, 454-461 (2005).
- 32 Landis, R. M. & Peart, D. R. Early performance predicts canopy attainment across life histories in subalpine forest trees. *Ecology* **86**, 63-72 (2005).
- 33 Brienen, R. & Zuidema, P. Programa manejo de bosques de la Amazonia Boliviana (PROMAB). Informe Tecnico No. 7. Anillos de crecimiento de árboles maderables en Bolivia: su potencial para el manejo de bosques y una guía metodológica. (Riberalta, Bolivia, 2003).
- 34 Poorter, L., Bongers, L. & Bongers, F. Architecture of 54 moist-forest tree species: Traits, trade-offs, and functional groups. *Ecology* **87**, 1289-1301 (2006).
- 35 Mostacedo, B., Justiniano, J., Toledo, M. & Fredericksen, T. *Guía Dendrológica de especies forestales de Bolivia*. (BOLFOR, 2003).
- 36 Williams, L. J., Bunyavejchewin, S. & Baker, P. J. Deciduousness in a seasonal tropical forest in western Thailand: Interannual and intraspecific variation in timing, duration and environmental cues. *Oecologia* **155**, 571-582 (2008).
- 37 Lemmens, R. H. M. J., Louppe, D. & Oteng-Amoako, A. A. *Plant Resources of Tropical Africa: Timbers 2*. (PROTA Foundation, 2012).
- 38 Poorter, L., Bongers, F., Kouamé, F. N. & Hawthorne, W. D. *Biodiversity of West African Forests. An ecological atlas of woody plant species*. (CABI International, 2004).
- 39 Worbes, M. How to measure growth dynamics in tropical trees - A review. *IAWA Journal* **16**, 337-351 (1995).